A 7-Switch Hybrid Energy Harvesting and Power Management System with Cascade Conversion Rejection for Both AC and DC Sources

Xiudeng Wang
Key Laboratory of Analog Integrated Circuits
Xidian University
Xi'an, China
wangxiudeng@xidian.edu.cn

Chenyu Pan
Key Laboratory of Analog Integrated Circuits
Xidian University
Xi'an, China
23211215107@stu.xidian.edu.cn

Libo Qian
Key Laboratory of Analog Integrated Circuits
Xidian University
Xi'an, China
qianlibo@ xidian.edu.cn

Yinshui Xia
Faculty of Electrical Engineering and Computer Science
Ningbo University
Ningbo, China
xiayinshui@nbu.edu.cn

Huakang Xia
Faculty of Electrical Engineering and Computer Science
Ningbo University
Ningbo, China
xiahuakang@nbu.edu.cn

Zhangming Zhu
Key Laboratory of Analog Integrated Circuits
Xidian University
Xi'an, China
zmyh@263.net

***Abstract*—This paper presents a 7-switch hybrid energy harvester with cascaded conversion rejection, enabling simultaneous AC and DC energy harvesting through a single-stage architecture. An envelope scale extraction (ESE) MPPT is employed for AC source, while a fractional open-circuit voltage (FOCV) MPPT is used for DC source. The proposed bridgeless synchronized switch harvesting on inductor (BL-SSHI) interface eliminates the rectifier bridge and capacitor, significantly enhancing power extraction of the piezoelectric source. Notably, the extraction signal of the piezoelectric source is multiplexed as the sampling signal for FOCV, enabling clock-free operation for photovoltaic (PV) energy harvesting. Fabricated in a 0.18 µm CMOS process, the harvester achieves a peak MPPT efficiency of 99.3% and an end-to-end efficiency of 88%, while maintaining an ultra-low quiescent current of 24 nA. The BL-SSHI interface further improves power enhancement, achieving up to 9.8× the output power of a full-bridge rectifier.**

Keywords—hybrid energy harvester, MPPT, piezoelectric transducer, bridgeless rectifier

I. Introduction

Energy harvesting (EH) has emerged as an innovative approach for powering low-power applications such as battery-powered apparatus and wireless sensor nodes. Since most energy sources available in the ambient environment are stochastic, it is often desirable to simultaneously harvest multiple types of energy sources, such as vibration, light, and RF radiation, for enhancing the output power and overall reliability of the EH system. Several hybrid EH solutions have been reported to harvest energy from different environmental sources. The hybrid system reported in [1] simultaneously harvested light, vibration, and RF energy with a single shared inductor. In [2], a serial stack resonance architecture was proposed to combine vibration, light, and thermal energy. In [3], a hybrid EH system combined vibration, light, and biofuel cells to deliver power to three loads. However, these systems adopted cascaded architectures, comprising rectification, MPPT, and regulation, and usually suffered from low end-to-end efficiency. The work in [4] achieved single-stage power delivery for multiple inputs and multiple outputs, and energy extraction from three energy sources. However, the absence of Maximum Power Point Tracking (MPPT) for piezoelectric energy harvesting (PEH) significantly restricts its power output capacity, as illustrated in the top left of Fig. 1. A recent hybrid harvester with MPPT for both AC and DC sources has been proposed [5], but the MPPT for its PEH operates at the rectified voltage, leading to a two-stage conversion and efficiency degradation, as shown in the top right of Fig. 1.

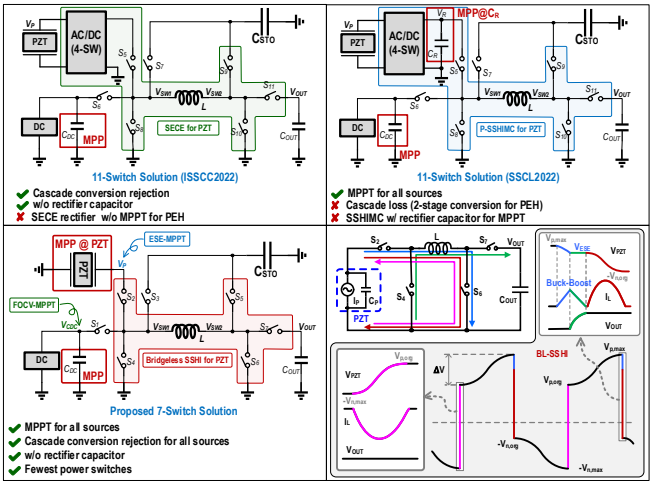

Fig. 1. 11-switch hybrid energy harvesting solution (top); proposed 7-switch solution with BL-SSHI (bottom).

To overcome these limitations, this paper proposes a 7-switch hybrid energy harvester that integrates a Bridgeless Synchronized Switch Harvesting on Inductor (BL-SSHI) interface for PEH, a buck-boost converter for Photovoltaic Energy Harvesting (PV-EH), and a buck converter for stored energy to power load, as shown in the bottom of Fig. 1. Capitalizing on the topological equivalence between the BL-SSHI and buck-boost converter, the proposed hybrid energy harvester implements an innovative switch-multiplexing strategy. This approach strategically shares switching components between the two converter topologies, achieving

This work was supported in part by the National Natural Science Foundation of China under Grant 62222406, Grant 62131010, Grant U22A2013, Grant 62271275, the China Postdoctoral Science Foundation under Grant 2023M742733 and the Postdoctoral Fellowship Program of CPSF under Grant GZB20230560, and in part by the Zhejiang Provincial Natural Science Foundation of China under Grant QN25F040020, Grant LDT23F0402, and in part by the Fundamental Research Funds for the Central Universities under Grant ZYTS25037. *(Corresponding author: Libo Qian)*

a dramatic reduction in power switch count while preserving full system. Furthermore, an envelope scale extraction (ESE) MPPT is implemented on piezoelectric transducer (PZT) terminal, which eliminates the rectifier capacitor and reduces conversion stages, thereby enhancing end-to-end efficiency.

II. Theoretical Analysis and Implementation

The characteristic waveforms of the BL-SSHI are shown at the bottom right of Fig. 1. At the positive peak of the open-circuit voltage of the PZT, the interface circuit enters into T_{ON} phase, switches S_2 and S_6 are turned on and the clamped capacitor C_P of the PZT charges the inductor L, and thus V_p decrease accordingly. When V_P drops to V_{ESE}, the interface enters into T_{OFF} phase, S_4 and S_7 are turned on, while S_2 and S_6 are turned off. Then, the inductor begins to discharge its energy to the load. Completion of this phase marks the end of energy extraction. Following energy extraction, a voltage inversion phase is executed by reactivating S_2 and S_6, inverting C_P's voltage polarity. In contrast to the positive half-cycle, the negative half-cycle's peak exclusively activates the voltage inversion. Based on the above analysis, it is observed that the proposed BL-SSHI integrates the rectifier and the DC-DC converter into one stage of conversion, thereby avoiding cascaded conversion. Furthermore, the PE energy is extracted to the output by the Buck-Boost conversion, thus, the proposed BL-SSHI interface is load independent.

To ensure maximum output power is achieved, a MPPT method is introduced in the proposed interface. The output power of the BL-SSHI can be expressed as:

$$P_{BL-SSHI} = \frac{1}{2} f C_p V_{p,\max}^2 (1-k^2) \tag{1}$$

where the ESE factor k represents the ratio of the extraction voltage V_{ESE} to the peak voltage $V_{p,max}$ and $V_{p,max}$ can be further expressed as:

$$V_{p,\max} = \frac{\Delta V(1+\gamma)}{1-k\gamma^2} \tag{2}$$

where ΔV and γ are the increment of the open-circuit voltage of the PZT during half a cycle and inversion factors, respectively. Substituting Eq. (2) into Eq. (1) gives:

$$P_{BL-SSHI} = \frac{1}{2} f C_p \Delta V^2 \frac{(1+\gamma)^2(1-k^2)}{(1-k\gamma^2)^2} \tag{3}$$

The optimal ESE factor k_{opt} that maximizes the output power is derived by taking the derivative of the expression in Eq. (3) with respect to k:

$$k_{opt} = \gamma^2 \tag{4}$$

The corresponding maximum output power is written as:

$$P_{BL-SSHI,\max} = \frac{1}{2} f C_p \Delta V^2 \frac{1+\gamma}{(1-\gamma^2)(1-\gamma)} \tag{5}$$

To visualize the relationship between the output power of the BL-SSHI versus the ESE factor k, Eq. (3) is plotted as a graphical presentation, as shown in Fig. 2(a). Furthermore, the output powers of different interfaces are plotted versus the rectified voltage V_R in Fig. 2(b). While the Synchronous Electrical Charge Extraction (SECE) technique demonstrates inherent advantages in load-independent, it inherently faces limitations in its maximum power output. Conversely, the conventional SSHI topology excels in achieving high peak power output. However, this performance advantage comes at the expense of sensitivity to load variations, specifically, deviations from the optimal rectified voltage result in drastic reductions in power output. The proposed BL-SSHI addresses this critical trade-off between output power and load independence.

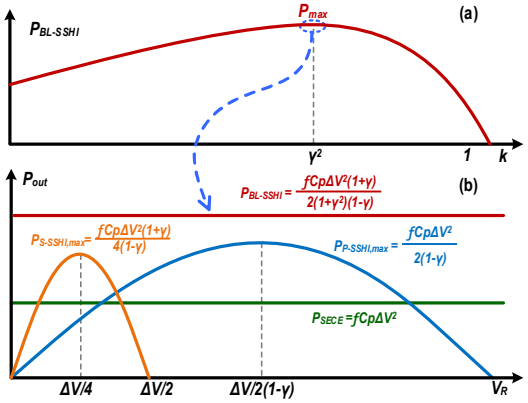

Fig. 2. (a) BL-SSHI output power versus extraction scaling factor k. (b) Output power versus rectified voltage V_R for several interfaces.

According to the principle of the BL-SSHI operation, the PEH circuit remains open-circuit during most of the time and extracts energy only when the open-circuit voltage reaches the peak. The PV-EH occurs at during non-piezoelectric peak moments. A fractional open-circuit voltage (FOCV) based MPPT method is adopted for the PV-EH. At piezoelectric peak moments, the PV-EH circuit operates in sampling phase to sense the PV's open-circuit voltage, as shown in Fig.3. By aligning the PZT's inductor access periods with FOCV sampling phases, this design inherently resolves potential resource conflicts that could arise from concurrent inductor utilization by two energy sources, achieving the harvesting of two types of energy within a single vibration cycle. Furthermore, with this design, the extraction signal of the piezoelectric energy can be multiplexed as the sampling signal for FOCV, enabling clock-free operation for the PV-EH.

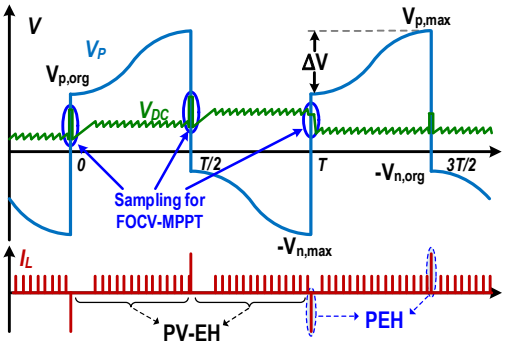

Fig. 3. Characteristic waveforms of proposed hybrid harvester.

Fig. 4 shows the block diagram of the proposed hybrid energy harvester, which is primarily composed of a power stage and a control stage. The power stage features seven power switches. The power switches that experience source-drain voltage variations are configured with Dynamic Body Bias (DBB), which effectively mitigates leakage currents caused by body diode conduction in these specific devices. The control stage integrates multiple specialized controllers and auxiliary modules, meticulously designed to optimize EH efficiency. Core components include: PZT Controller, PV Controller, Load Controller, Switch Logic Unit and Auxiliary Support Block. The PZT controller is composed of

Peak Detector (PKD), Reverse Current Detector (RCD), envelope extractor, and ESE-MPPT controller. The PV controller consists of an FOCV-MPPT controller, sampling signal extraction module. The load controller is a buck converter based on Pulse Skipping Modulation (PSM). Logic controller includes cascade conversion rejection-based power path selector and signal logic. Auxiliary modules include Zero Crossing Detector (ZCD), voltage reference, and current bias.

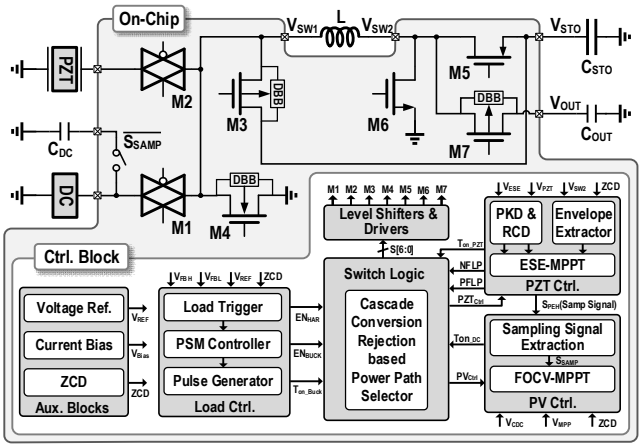

Fig. 4. System architecture of the proposed hybrid energy harvester.

The proposed hybrid harvester employs an asynchronous event driven control mechanism to minimize static power consumption. The control logic is triggered by multiple events, including PKD, ESE-MPPT, FOCV-MPPT, ZCD, RCD and comparison signal for load voltage detection.

The circuit implementation of the ESE-MPPT for BL-SSHI interface is illustrated in Fig. 5. The active diode (AD) and capacitor form a peak detection network that captures and maintains the maximum voltage excursions from the PZT. Simultaneously, the resistor divider network taps this stored energy to produce the envelope extraction voltage V_{ESE} ($V_{ESE} = \gamma^2 \times V_{p,max}$). In the PEH process, the open-circuit voltage of the PZT (V_P) gradually decreases, and when it drops to V_{ESE}, the comparator output a high signal to reset the D flip-flop and complete the energy extraction from PZT. This design achieves the MPPT for PEH mentioned above.

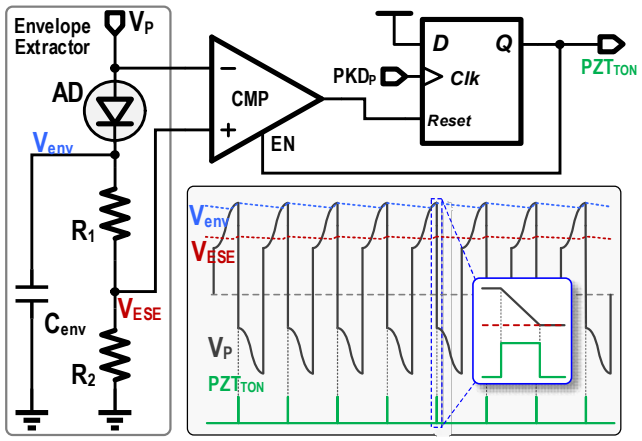

Fig. 5. Implementation of ESE-MPPT.

III. Measurement Results

The proposed hybrid energy harvesting and management system is fabricated in a 180 nm CMOS process with a core area of 0.91 mm^2. As shown in the Fig 6 (a), power switches constitute the primary component occupying chip area. This indicates that reducing the number of switches would lead to a substantial reduction in chip dimensions. The off-chip device main contains a 100-µH inductor, three capacitors (C_{STO}=220µF, C_{OUT}=22µF, C_{DC}=4.7µF).

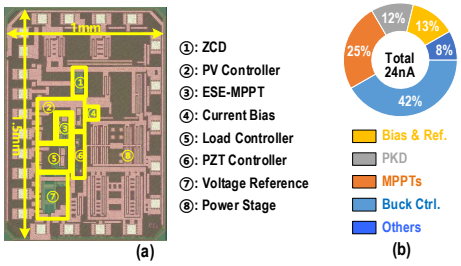

Fig. 6. (a) Chip micrograph and (b) quiescent current breakdown.

To enable low-power operation, this work employs an event-driven asynchronous clock control scheme with power gating. The quiescent current of the harvester is as low as 24 nA as shown in Fig. 6(b).

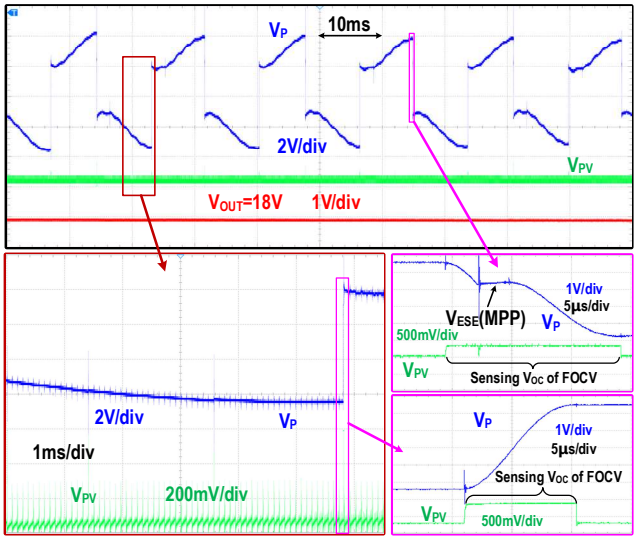

Fig. 7. Measured representative voltage waveforms.

Fig. 7 shows the measured voltage waveforms. it is observed that during piezoelectric energy extraction, the voltage V_P first falls partially, and then maintains a certain level (V_{ESE}) for a period of time, and finally completes the voltage inversion, the result indicates that the MPPT for PEH is achieved. In the meantime, the PV energy harvester is triggered to enter the sampling phase and the open-voltage (V_{OC}) of PV cell is sensed. During the idle intervals of extracting piezoelectric energy, the PV energy is extracted using FOCV-MPPT.

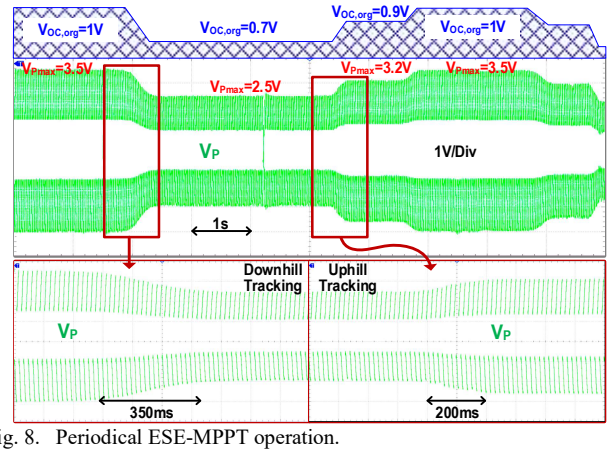

Fig. 8. Periodical ESE-MPPT operation.

Fig. 8 illustrates the variation of V_P voltage of the PZT with the vibration amplitude under continuous periodic vibration conditions. From the zoomed-in graphs of uphill and downhill tracking, it can be found that after adopting the proposed ESE-MPPT method, the V_P voltage is able to follow the vibrations in real time. Once the vibration amplitude stabilizes, the V_P voltage can immediately return to a stable state.

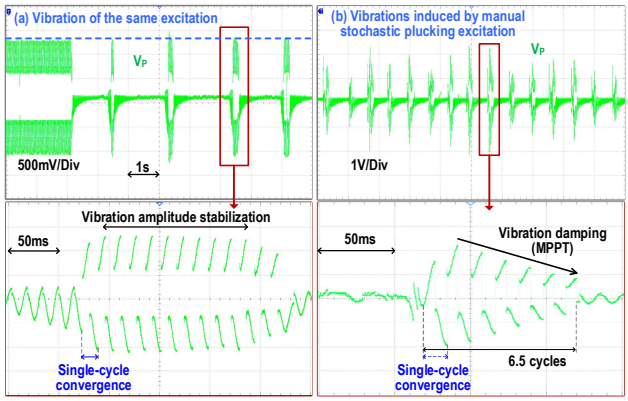

Fig. 9. Shock vibration with (a) the same excitation, (b) manual stochastic plucking excitation.

Fig. 9(a) exhibits the measured tracking results of the MPPT under a shock vibration scenario with constant excitation. From the graph at the top, it is observed that the V_P voltage rapidly tracks the MPP and attains an amplitude level compared to those maintained at periodic vibration. The zoom-in graph at the bottom reveals that from start up to reaching MPP, the PEH circuit requires only one cycle. It demonstrates the rapid response speed of the ESE-MPPT. Fig. 9(b) shows the measured tracking results of the MPPT during PZT under a random vibration scenario. This random vibration is generated by manually plucking the cantilever beam. Since the plucking is an instantaneous excitation, the vibration decays gradually. As shown in the zoom-in graph at the bottom, the V_P voltage is constantly tracking the MPP and diminishes gradually with the attenuation of vibration amplitude in 6.5-cycle. Experimental validation demonstrates that the proposed ESE-MPPT technique enables seamless maximum power extraction in various vibration scenarios.

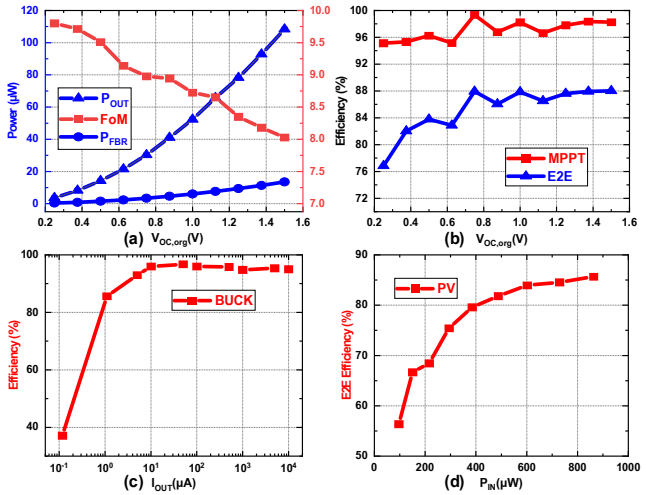

Fig. 10. (a) P_{OUT} of PEH versus $V_{OC,org}$, (b) MPPT and E2E efficiency of PEH, (c) efficiency of Buck, (d) E2E efficiency of PV-EH.

Fig. 10(a) illustrates the output power of the BL-SSHI, the maximum output power of the FBR, and the Figure of Merit (FoM) across varying vibration amplitudes. Within the measured range, the output power of the BL-SSHI maintains more than 8 times that of the FBR, with a maximum of 9.8 times. Fig. 10(b) shows the MPPT and end-to-end efficiency of PE energy harvesting with different vibration amplitudes, where the highest MPPT and end-to-end efficiency reach 99.3% and 88%, respectively. Fig. 10(c) presents the power conversion efficiency (PCE) of the buck converter with a maximum of 96.7%. Fig. 10(d) illustrates the end-to-end efficiency of PV energy harvesting which is up to 85.7%.

Table I summarizes the performance comparison of state-of-the-art hybrid energy harvesters. With single-stage conversion and dual-MPPT methods, the proposed hybrid harvester achieves simultaneous harvesting of both AC and DC energy with only seven switches, with maximum end-to-end efficiencies of 88% and 85.7%, respectively. Additionally, the proposed BL-SSHI not only eliminates the rectifier capacitor, but also achieves a highest power enhancement, with test results indicating up to 9.8 times that of the FBR. Moreover, the proposed ESE-MPPT features a fast response speed and can achieve convergence within a single vibration cycle.

TABLE I. COMPARISON WITH STATE-OF-THE-ART WORKS

Publication	JSSC 2016 [1]	SSCL 2022 [5]	JSSC 2023 [2]	ISSCC 2022 [4]	This Work
Technology	180nm	180nm	180nm	65nm	**180nm**
Sources	AC & DC (PE&PV&RF)	AC & DC (PE&PV&BFC)	AC & DC (2- PE&PV&TEG)	AC & DC (PE&PV&TEG)	**AC & DC (PE&PV)**
C_p	N/R	18nF	100nF	N/R	**100nF**
Frequency	100Hz	N/R	25Hz	N/R	**59Hz**
Inductance	47μH	10μH	470μH	22μH	**100μH**
Rectifier Type	FBR	SSHIMC	SECE	SECE	**BL-SSHI**
Chip Dimension	1.1mm^2(core)	4mm^2	0.9mm^2(core)	3.1mm^2	**0.91mm^2(core)**
Rectifier Capacitor	Required	Required	Not Required	Not Required	**Not Required**
MPPT Technique	FOCV	P&O	FOCV	FOCV	**ESE & FOCV**
Dedicated Clock	Required	Required	Not Required	Required	**Not Required**
Quiescent Power	18nA	N/R	N/R	32nA	**24nA**
PEH MPPT	YES	YES	NO	NO	**YES**
PEH Conversion Stages	3-Stage	2-Stage	2-Stage (w/o MPPT)	1-Stage (w/o MPPT)	**1-Stage**
Converter Topology	4-Input/2-Out 12-SW+RF Rect.	4-Input/4-Out 14-SW	4-Input/1-Out 14-SW	4-Input/5-Out 15-SW	**3-Input/2-Out 7-SW**
Regulated V_{OUT}	PFM	PFM	N/A	PFM&PWM	**PSM**
Peak MPPT Efficiency	>95%	95%	<95%	N/R	**99.3%**
Peak Efficiency	PV: 85% (PCE) PE: 87% (PCE)	STO: 87% (PCE)	PV: 84% (PCE) PE: 76.5% (PCE)	PV: 81.5% (PCE) PE: N/R STO: 81% (PCE)	**PV: 85.7% (E2E) PE: 88% (E2E) STO: 96.7% (PCE)**
FoM	< 1	5.7×	2.3×	3.2×	**9.8×**

REFERENCES

[1] G. Chowdary, A. Singh, and S. Chatterjee, "An 18 nA, 87% Efficient Solar, Vibration and RF Energy Harvesting Power Management System With a Single Shared Inductor," in IEEE JSSC, vol. 51, no. 10, pp. 2501-2513, Oct. 2016.

[2] X. Wang, Y. Xia, Z. Zhu, G. Shi, H. Xia, Y. Ye, Z. Chen, L. Qian, and L. Liu, "Configurable Hybrid Energy Synchronous Extraction Interface With Serial Stack Resonance for Multi-Source Energy Harvesting," in IEEE JSSC, vol. 58, no. 2, pp. 451-461, Feb. 2023.

[3] S. S. Amin and P. P. Mercier, "MISIMO: A Multi-Input Single-Inductor Multi-Output Energy Harvester Employing Event-Driven MPPT Control to Achieve 89% Peak Efficiency and a 60,000× Dynamic Range in 28nm FDSOI," IEEE ISSCC, pp. 144-145, Feb. 2018.

[4] S. Li, X. Liu, and B. H. Calhoun, "A 32nA Fully Autonomous Multi-Input Single-Inductor Multi-Output Energy-Harvesting and Power-Management Platform with 1.2×105 Dynamic Range, Integrated MPPT, and Multi-Modal Cold Start-Up," IEEE ISSCC, pp. 472–473, Feb. 2022.

[5] S. Chamanian and P. P. Mercier, "MIPSIMO: A Multi-Input Piezo-Adaptive Single-Inductor Multi-Output Energy Harvester Achieving Using a Shared Inductor With an Integrated Analog Computer Achieving 95% MPPT Efficiency," in IEEE SSCL, vol. 5, pp. 222-225, 2022.